for the bubbly flow. The sampling time was 30 to 60 s. The tip of the probe was made of 0.1 mm diameter stainless-steel wire whose outer surface was covered with polyester insulation of about 0.01 mm thickness. The probe, mounted on a micrometer head, was arranged in a holder ⑨ that could be rotated about the tube axis, to permit measurements of distribution to be made in any direction across the tube cross section at measuring position. The holder was installed at 100 tube diameters downstream from the bend exit ($L/D=100$), because nearly fully-developed downward flow was attained there as presented in APPENDIX.

III. EXPERIMENTAL RESULTS AND DISCUSSION

1. Void Distribution and Average Void Fraction

Photographs of typical flow regimes observed in the downcomer with a 16 mm inside diameter are shown in **Photo. 1**(a)~(f). Further, some typical examples of the void distribution measured for these flow regimes are shown in **Fig. 2**(a) for $D=16$ mm, and Fig. 2(b) for $D=24$ mm. The cross section average void fraction was obtained by numerical integration of the measured local void fraction over the whole cross section. Liquid droplets occur in high velocity annular flow. The amount of the liquid entrainment can not catch by means of the conductance needle probe used. However, the cross-sectional area occupied by entrained droplets in the tube is very small compared with that occupied by other parts (liquid film and gas). For this reason a participation of entrained droplets with respect to the average void fraction can be neglected.

(1) Bubbly Flow

For the downward bubbly flow, bubbles have a tendency to move toward the center of the tube because of the lift force acting on bubbles caused by the velocity gradient in

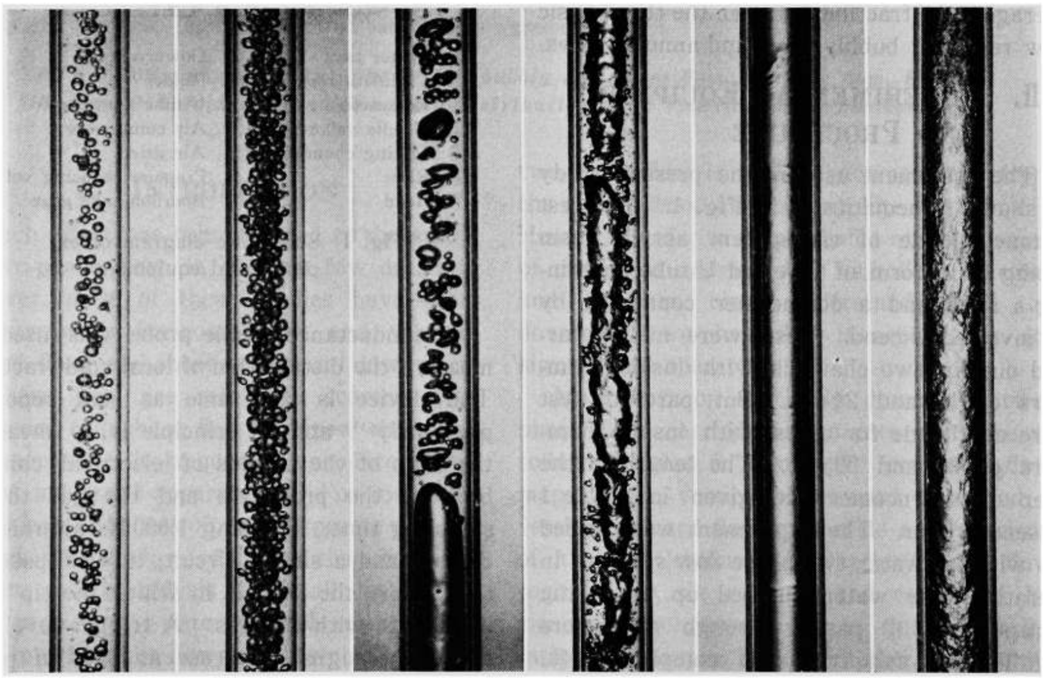

(a) (b) (c) (d) (e) (f)

(a)	Bubbly	$j_L=-1.49$ m/s,	$j_G=-0.10$ m/s	(d)	Slug (churn)	$j_L=-1.0$ m/s,	$j_G=-1.24$ m/s
(b)	Bubbly	$=-1.49$,	$=-0.332$	(e)	Falling film	$=-0.091$,	$=-1.24$
(c)	Slug	$=-0.664$,	$=-0.332$	(f)	Annular drop	$=-1.0$,	$=-14.1$

Photo. 1(a)~(f) Flow regime in downward flow ($D=16$ mm)

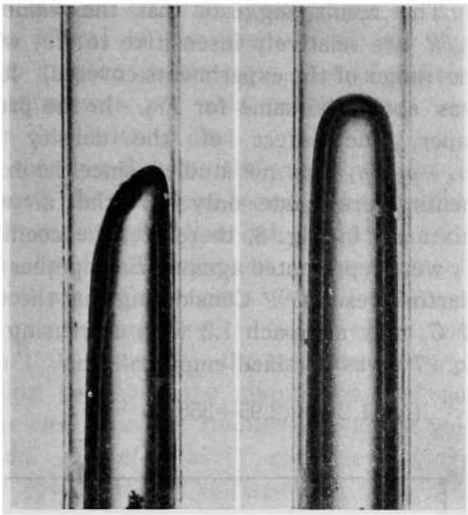

(a) $j_L=-0.29$ m/s (b) $j_L=0$

Photo. 2(a),(b) Shape of isolated bubble (D=32 mm)

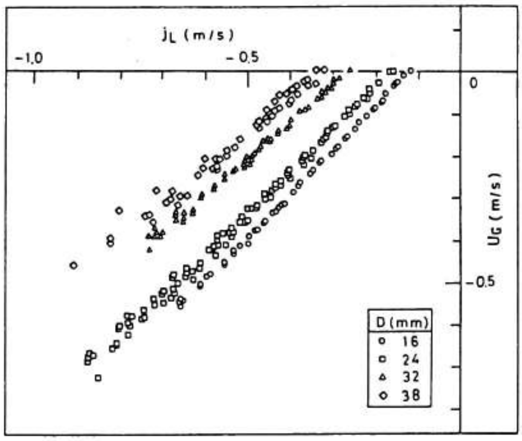

Fig. 5 Descending bubble velocity (isolated bubble)

the downward slug flow and the isolated bubble flow can be represented by Eq. (1).

The drift velocity V_{Gj} for the slug flow is generally expressed as

$$V_{Gj}=C_1\sqrt{gD(\rho_L-\rho_G)/\rho_L}. \qquad (5)$$

From results of Figs. 4 and 5, the values of C_0 and C_1, which were given in **Table 1**, were obtained. As be seen there, the difference in bubble velocity between the slug flow and the isolated bubble flow is relatively small, so that the contribution for the bubble velocity of small bubbles between gas slugs in the slug flow can not be found from these results.

Table 1 Distribution parameter and drift velocity coefficient

D(mm)	16		24		32	36
Flow	Slug flow	Isolated bubble	Slug flow	Isolated bubble	Isolated bubble	Isolated bubble
C_0	1.02	1.04	0.97	1.0	0.89	0.90
C_1	0.39	0.31	0.36	0.32	0.41	0.49
$C_1(j_L=0)$		0.32~0.33		0.33~0.34	0.34~0.36	0.35~0.39
L(m)	3.0	2.65	4.2	3.12	5.16	4.8
T(°C)	9~13		7~11		9~12	12~13

The shape of a gas slug in vertical upward flow is symmetric with respect to the tube axis, and the velocity depends upon both the nose shape of bubble and the profile of liquid velocity, when gravity and inertia force govern the flow, being hardly affected by the length of the bubble. Nicklin *et al.*[14] have shown that the distribution parameter C_0 can be identical with the ratio of maximum to mean velocity: $C_0\cong 1.2$, and the coefficient C_1 is about 0.35 for the upward flow. Likewise in downward flow, the bubble velocity would be influenced by the shape of the bubble, especially that of tail part and its location relative to the velocity profile in the liquid slug. A peak on profile of local void fraction seen in Fig. 2(a) and (b) appears to show a location of the tail end of the large bubbles.

The coefficient C_0 is approximately the ratio of the bubble velocity observed from